PNAS RESEARCH ARTICLE | EVOLUTION

Discovery of prolactin-like in lamprey: Role in osmoregulation and new insight into the evolution of the growth hormone/prolactin family

Ningping Gong[a,1], Diogo Ferreira-Martins[b,c,d], Jessica L. Norstog[b,e], Stephen D. McCormick[b,c], and Mark A. Sheridan[a,1]

Edited by Lynn Riddiford, University of Washington, Friday Harbor, WA; received July 18, 2022; accepted August 8, 2022

We used a representative of one of the oldest extant vertebrate lineages (jawless fish or agnathans) to investigate the early evolution and function of the growth hormone (GH)/prolactin (PRL) family. We identified a second member of the GH/PRL family in an agnathan, the sea lamprey (*Petromyzon marinus*). Structural, phylogenetic, and synteny analyses supported the identification of this hormone as prolactin-like (PRL-L), which has led to added insight into the evolution of the GH/PRL family. At least two ancestral genes were present in early vertebrates, which gave rise to distinct GH and PRL-L genes in lamprey. A series of gene duplications, gene losses, and chromosomal rearrangements account for the diversity of GH/PRL-family members in jawed vertebrates. Lamprey PRL-L is produced in the proximal pars distalis of the pituitary and is preferentially bound by the lamprey PRL receptor, whereas lamprey GH is preferentially bound by the lamprey GH receptor. Pituitary PRL-L messenger RNA (mRNA) levels were low in larvae, then increased significantly in mid-metamorphic transformers (stage 3); thereafter, levels subsided in final-stage transformers and metamorphosed juveniles. The abundance of PRL-L mRNA and immunoreactive protein increased in the pituitary of juveniles under hypoosmotic conditions, and treatment with PRL-L blocked seawater-associated inhibition of freshwater ion transporters. These findings clarify the origin and divergence of GH/PRL family genes in early vertebrates and reveal a function of PRL-L in osmoregulation of sea lamprey, comparable to a role of PRLs that is conserved in jawed vertebrates.

growth hormone | prolactin | evolution of hormones | osmoregulation | metamorphosis

The growth hormone (GH)/prolactin (PRL) family in jawed vertebrates (gnathostomes) includes GH and PRL, both of which have been found in all gnathostome lineages (1–4), prolactin 2 (PRL2), which has been identified in nonmammalian species (1, 5, 6), and somatolactin (SL), which has been identified exclusively in ray-finned fishes (1, 7). The family appears to have arisen from a common ancestor and constitutes a gene family within the class-I cytokine superfamily (1, 8). The GH/PRL family shares similarities in gene structure, generally being composed of five to six exons, as well as in protein tertiary structure, featuring four helices (6, 8, 9).

The appearance of a GH-like cytokine dates back to the emergence of chordates, and a functional GH-like homolog has been characterized in a protochordate, the lancelet *Branchiostoma japonicum* (10). A GH-like protein has been identified in the pituitary of both lineages of extant jawless vertebrates (agnathans): hagfish and lamprey (11, 12). To date, however, family members other than GH (i.e., PRL, PRL2, and SL) have not been found in any agnathan or protochordate (1, 2, 6).

One evolutionary scenario holds that GH is the ancestor of the gene family in vertebrates (12) and that PRL and SL may have arisen after the divergence of the agnathan and gnathostome lineages (2, 12, 13). An alternative scenario was proposed based on phylogenetic and synteny analyses, suggesting an earlier timing for divergence of the gene family and the presence of a triplet of GH, SL, and an ancestral PRL/PRL2 in an early vertebrate ancestor (1). Both scenarios provide an explanation for the origins of the GH/PRL family regardless of the number of whole-genome duplication events, either only one round (1R) (14–16) or two successive rounds (1R and 2R) (15, 17, 18), that basal vertebrates underwent prior to the divergence of lamprey and jawed vertebrates. Genomic comparisons among the protochordate, Florida lancelet (*B. floridae*) (14), lampreys (16, 17), and gnathostome species (14, 16) recently provided new insight into the genome duplication events of early vertebrates. Based on these analyses, the 1R event preceded divergence of lamprey and jawed vertebrate lineages. Lamprey subsequently went through large-scale duplication events after 1R (14–16), while gnathostome stem lineages went through a series of chromosomal fusions and rearrangements that preceded the 2R duplication event in jawed vertebrates (2Rjv) (14, 16).

Significance

Jawless fishes (agnathans), one of the oldest groups of living vertebrates, provide a unique opportunity to study the origin and divergence of genes as well as the evolution of hormone function. We identified in an agnathan a second member of the growth hormone (GH)/prolactin (PRL) family, characterized as prolactin-like (PRL-L), and propose a new model for the evolution of the GH/PRL gene family. At least two ancestral genes were present in ancestral vertebrates, with a series of gene duplications, gene losses, and chromosomal rearrangements accounting for the various GH/PRL-family members in jawed vertebrates. PRL-L plays a role in freshwater acclimation of the sea lamprey, a role which is conserved for PRL in jawed vertebrates.

Author affiliations: [a]Department of Biological Sciences, Texas Tech University, Lubbock, TX 79409; [b]Eastern Ecological Science Center, S.O. Conte Anadromous Fish Research Laboratory, US Geological Survey, Turners Falls, MA 01376; [c]Department of Biology, University of Massachusetts, Amherst, MA 01003; [d]Centro de Investigação Marinha e Ambiental, University of Porto, Matosinhos, 4450-208 Portugal; and [e]Graduate Program in Organismic and Evolutionary Biology, University of Massachusetts, Amherst, MA 01003

Author contributions: N.G., S.D.M., and M.A.S. designed research; N.G., D.F.M., J.L.N., and S.D.M. performed research; N.G. and M.A.S. analyzed data; and N.G. and M.A.S. wrote the paper.

The authors declare no competing interest.

This article is a PNAS Direct Submission.

[1]To whom correspondence may be addressed. Email: mark.sheridan@ttu.edu or ningping.gong@ttu.edu.

This article contains supporting information online at http://www.pnas.org/lookup/suppl/doi:10.1073/pnas.2212196119/-/DCSupplemental.

Published September 26, 2022.

The study of agnathans, including sea lamprey (*Petromyzon marinus*) (17), Arctic lamprey (also known as Japanese river lamprey; *Lethenteron camtschaticum*) (16, 18), Far Eastern brook lamprey (*L. reissneri*) (19), and inshore hagfish (*Eptatretus burger*) (20), provides a unique opportunity to clarify the origin and divergence of the GH/PRL gene family, because of their pivotal phylogenetic positions and recent availability of genomic datasets. Sea lamprey are particularly interesting because of their anadromous life cycle, consisting of a freshwater larval phase, metamorphic transformers, postmetamorphic juveniles that migrate to sea, marine parasitic lamprey, and sexually mature adults that return to fresh water to spawn (21).

In teleosts, GH and PRL have distinct roles in osmoregulation (22), but such roles have never been determined in agnathans, to our knowledge. Sea lamprey GH is expressed in the proximal pars distalis (PPD) of the pituitary (12, 23, 24). Removal of the PPD resulted in a failure to complete metamorphosis (arrested in stage 3) in *Geotria* lamprey (25). However, the hormones identified in the PPD, including GH and two glycoprotein hormones, do not appear to be involved (23, 24). Thus, an unknown pituitary factor that mediates metamorphic transformation and osmoregulation has yet to be discovered. Given the recent discovery of two distinct receptors that are characterized as orthologs of GH receptors (GHRs) and PRL receptors (PRLRs) in sea lamprey (26), in addition to the well-characterized role of PRL in regulating ion uptake essential to freshwater (FW) acclimation of teleosts (27) and of PRLs in metamorphosis of amphibians (28), we predicted the presence of a PRL-like (PRL-L) hormone in sea lamprey.

In this study, we identified and characterized a second member of the GH/PRL family in the pituitary of a representative agnathan, the sea lamprey, which is structurally similar to PRL/PRL2 of jawed vertebrates. Phylogenetic and synteny analyses support the identification of the gene as PRL-L and allowed us to propose a revised model for the early evolution of the GH/PRL gene family. Last, we determined that PRL-L plays a role in osmoregulation of sea lamprey.

Results

Characterization of the PRL-Like Gene in Pma. Following the cloning of a full-length complementary DNA (cDNA) from the pituitary of sea lamprey (*Petromyzon marinus* [Pma]), we identified a gene similar in structure to that of sea lamprey GH (Pma.GH) and to the GH/PRL gene family in reedfish (*Erpetoichthys calabaricus*; hereafter, Eca) and spotted gar (*Lepisosteus oculatus*; hereafter, Loc), all of which are composed of five to six exons (Fig. 1*A*). The predicted protein contains 255 amino acids with a molecular weight of ~26 kDa, and was modeled to have a four-helix tertiary structure using human PRL as template (Fig. 1*B*). The structural similarities suggest identification as sea lamprey PRL-L (Pma.PRL-L; accession no. OP265705). Modeling Pma.GH using human GH as template predicted a similar four-helix structure (Fig. 1*C*). Despite similar tertiary structure, Pma.PRL-L has low amino acid identity with Pma.GH (29%) and gnathostome PRLs and GHs (<27%). Sequence alignment (*SI Appendix*, Fig. S1) shows high similarity (~40%) in the C-terminal amino acids encoded by the last exon between Pma.PRL-L and fish PRL2, and four conserved Cys residues.

Phylogeny of the Vertebrate GH/PRL Family. Phylogenetic analysis using alignment of mature protein sequences without signal peptides shows that lamprey PRL-Ls and lamprey GHs appear in distinct branches, with the lamprey PRL-L branch clustering at the base of gnathostome GH branch, but without good support. The lamprey GH branch clusters at the intersection of the branches of lamprey PRL-L and gnathostome GH, and the stem leading to the SL, PRL, and PRL2 branches, with reliable support (89%) (Fig. 1*D*).

Chromosomal Mapping of Gene Families in the Vicinities of Pma.GH and Pma.PRL-L. Sixty genes in the vicinities of Pma.GH and Pma.PRL-L were queried against the genomes of Eca, elephant shark (*Callorhinchus milii*; hereafter, Cmi) and chicken (*Gallus*; hereafter, Gga), and representatives from the repertoires of these gene families were found to be mostly located on chromosomes (Chr, when reported with a number) bearing the various GH/PRL family members and related chromosomes (Fig. 2 and *SI Appendix*, Figs. S2 and S3).

Paralogs that arose after the divergence of lamprey and gnathostome lineages are identified on those chromosomes of Eca, Cmi, and Gga. Five pairs of paralogs are present on PRL-bearing Eca.Chr11 and Eca.Chr12 (Fig. 2); four of the five pairs are conserved on Cmi.Chr16 and PRL-bearing Cmi.Chr31 (*SI Appendix*, Fig. S2), but only a single pair remained on Gga.Chr14 and Gga.Chr2, likely due to additional chromosomal rearrangement on Gga.Chr2 and Gga.Chr1 (*SI Appendix*, Fig. S3). Notably, PRL is located on Eca.Chr11, but it is not on the syntenic Cmi.Chr16 and Gga.Chr14; instead, PRL is located on the paralogous Cmi.Chr31 and Gga.Chr2. More paralogs are identified in Eca, including two pairs on Eca.Chr4 and Eca.Chr16 and seven pairs on SL-bearing Eca.Chr9 and Eca.Chr17 (Fig. 2). Remarkably, synteny is conserved in comparisons of SL-bearing Eca.Chr9 with Cmi.Chr25 and Gga.Chr24, but SL is absent in Cmi and Gga (Fig. 2 and *SI Appendix*, Figs S2 and S3). Moreover, the paralogy group on Eca.Chr17 is absent in Cmi and Gga (Fig. 2), which perhaps links to the loss of SL.

Paralogs from the repertoires of the same gene families are identified in lamprey and jawed vertebrates. Eight pairs of paralogs are identified on PRL-bearing Eca.Chr11 and GH-bearing Eca.Chr14 (Fig. 2); these paralogs also are conserved on Cmi.Chr20 and Cmi.Chr16 (*SI Appendix*, Fig. S2), and five pairs are on Gga.Chr14 and Gga.Chr18 (*SI Appendix*, Fig. S3). Five of the eight gene families have paralogs in Pma on GH-bearing Pma.Chr3 and Pma.Chr37 (Fig. 2). Moreover, seven pairs of paralogs are identified in Pma on PRL-L-bearing Pma.Chr62 and Pma.Chr32; among them, four pairs are ancient paralogs that diverged prior to vertebrates (Fig. 2). These paralogy groups are mostly identified on Eca.Chr4 and SL-bearing Eca.Chr9 (Fig. 2), on Cmi.Chr4 and Cmi.Chr25 (*SI Appendix*, Fig. S2), and on PRL2-bearing Gga.Chr1 and Gga.Chr24 (*SI Appendix*, Fig. S3). The presence of these paralogs indicates a common genome duplication event likely shared by the Pma and the jawed vertebrates.

Chromosomal Rearrangements of the Neighboring Gene Families. Twenty-eight of the 29 gene families neighboring Pma.GH are rearranged onto the GH-bearing Eca.Chr14, PRL-bearing Eca.Chr11 and paralogous Eca.Chr12, and SL-bearing Eca.Chr9 and paralogous Eca.Chr17 (Fig. 2). Most of these genes are identified on the syntenic chromosomes in Cmi and Gga (*SI Appendix*, Figs. S2 and S3). Notably, Eca.GH is located on Eca.Chr14 with the gene families that are syntenic on Cmi.Chr20 and Gga.Chr18, whereas Cmi.GH and Gga.GH are located on Cmi.Chr23 and Gga.Chr27, respectively.

Mixtures of representatives from the 29 gene families neighboring Pma.GH and the 31 gene families neighboring Pma.PRL-L are observed on the PRL-bearing and SL-bearing chromosomes in Eca. Sixteen of the 29 gene families are located on the

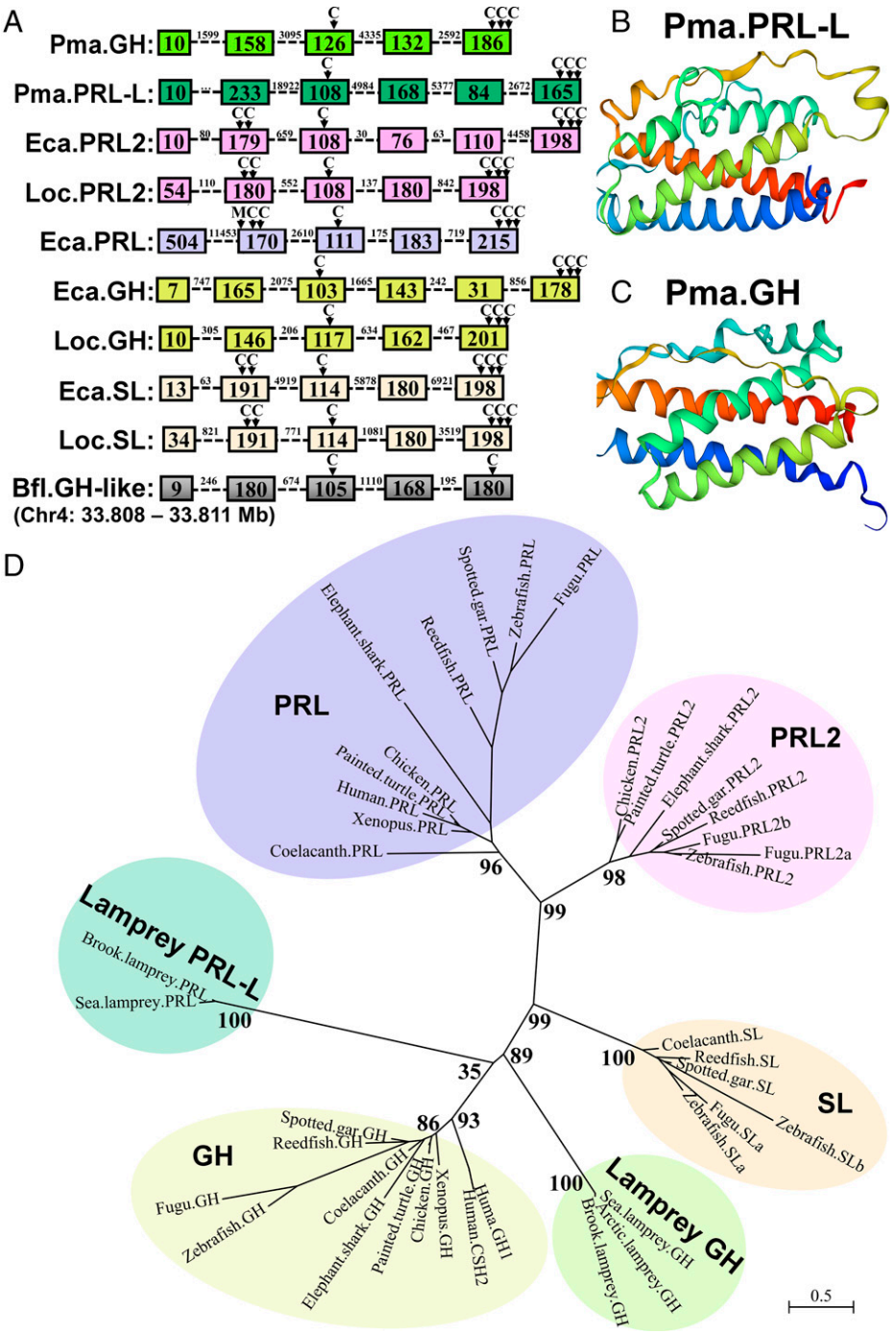

Fig. 1. Gene structure, tertiary protein structure, and phylogenetic analysis of lamprey PRL-L and GH. (*A*) Gene structures of Florida lancelet (Bfl) GH-like (GenBank no. XM_035815982.1); Pma PRL-L and Pma.GH; PRL, PRL2, GH, and SL of Eca; and PRL2, GH, and SL of Loc. Gene structure of Loc.PRL is unknown because of its absence in the current Loc genome dataset. The gene structures are composed of five to six exons and four to five introns; numbers refer to base pairs. M, Met residue; C, Cys residue. (*B* and *C*) SWISS-MODEL predicting the four-helix structures of Pma.PRL-L and Pma.GH, using human PRL (2q98.1.A) and human GH (1hwg.1.C) as templates, respectively. (*D*) Phylogenetic tree shows the branches of lamprey PRL-L and GH (sea lamprey, Arctic lamprey, and Far Eastern brook lamprey) and the clades of jawed-vertebrate GH, PRL, PRL2, and SL. The Arctic lamprey PRL-L sequence was incomplete and thus excluded in the phylogeny. Node support is reported as percentages.

PRL-bearing Eca.Chr11, mixing with three of the 31 gene families, while 10 of the 29 gene families are on the SL-bearing Eca.Chr9 and paralogous Eca.Chr17, mixing with 14 of the 31 gene families (Fig. 2). Similar mixing patterns also are present in the syntenic chromosomes of Cmi and Gga (*SI Appendix*, Figs. S2 and S3).

The rest of the 31 gene families neighboring Pma.PRL-L are mostly found on Eca.Chr4 (Fig. 2), Cmi.Chr4 (*SI Appendix*, Fig. S2), and PRL2-bearing Gga.Chr1 (*SI Appendix*, Fig. S3), whereas Eca.PRL2 and Cmi.PRL2 may have been rearranged to Eca.Chr1 (Fig. 2) and Cmi.Chr6 (*SI Appendix*, Fig. S2), respectively.

Characterization of Recombinant Pma.PRL-L and Pma.GH Proteins. *Escherichia coli*–produced recombinant Pma.PRL-L (rPRL-L) was ~26 kDa, similar in size to the predicted protein, in immunoblotting using the antibody to Pma.PRL-L (Ab-lPRL); preadsorption of the antibody (negative control) blocked the immunostaining of the 26-kDa band (Fig. 3*A*). Two bands

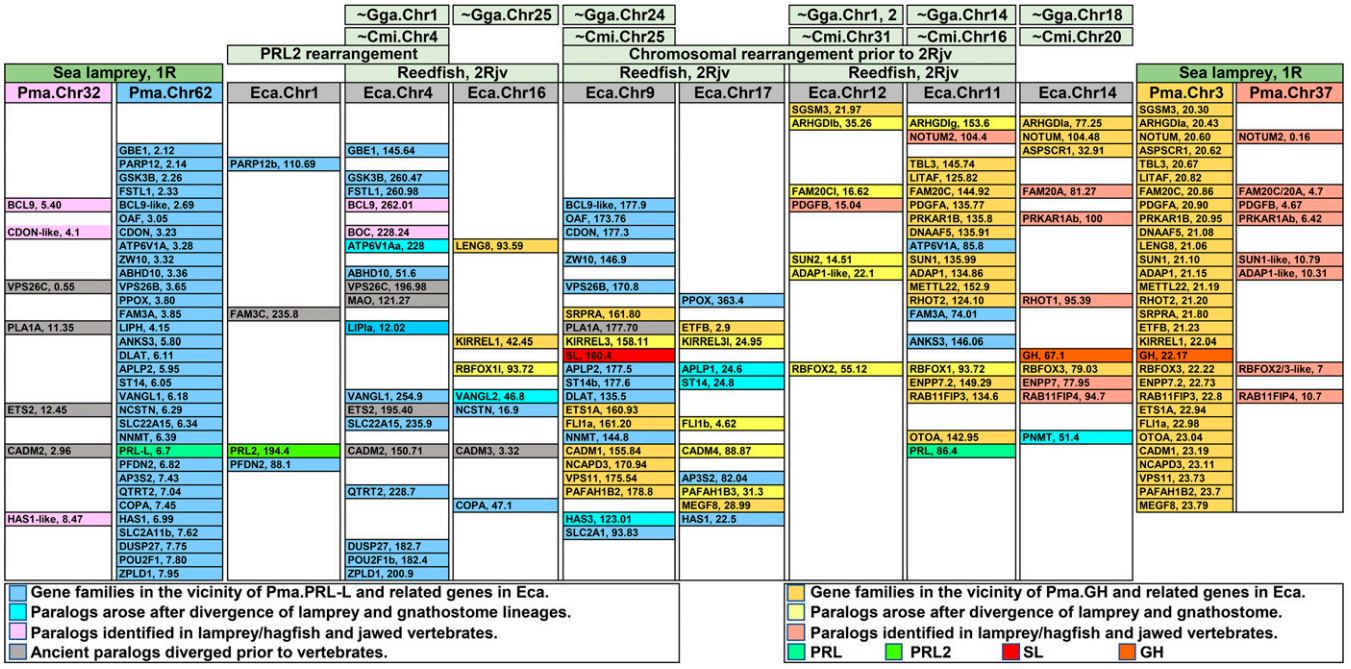

Fig. 2. Chromosomal comparison between Pma and Eca. Genes are denoted by their standard abbreviation in UniProKB; loci are reported in Mb. Chr, chromosome. Representatives from the 31 gene families in the vicinity of PRL-L on Pma.Chr62 (2.1 to 7.9 Mb; in blue) and the 29 gene families in the vicinity of GH on Pma.Chr3 (20.3 to 23.7 Mb; in yellow) are mostly identified in Eca and located on PRL2-bearing Chr1, Chr4, and paralogous Chr16; SL-bearing Chr9 and paralogous Chr17, Chr12, and paralogous PRL-bearing Chr11; and GH-bearing Chr14. Paralogs in Eca: two pairs on Chr4 and Chr16, seven pairs on Chr9 and Chr17, and five pairs on Chr11 and Chr12, which arose after divergence of lamprey and gnathostome lineages, likely in the event of 2Rjv. Six pairs of paralogs are on PRL-bearing Eca.Chr11 and GH-bearing Eca.Chr14, and the paralogs from the same gene families also are identified on GH-bearing Pma.Chr3 and Pma.Chr37. Seven pairs of paralogs are identified on Pma.Chr62 and Pma.Chr32, and the paralogs from the same gene families also are identified on Eca.Chr4 and SL-bearing Eca.Chr9. Among them, four pairs are ancient paralogs that diverged prior to vertebrates. Chromosomal rearrangements include fusion and mixing that may have occurred on SL-bearing Eca.Chr9, Eca.Chr17, and PRL-bearing Eca.Chr11, and rearrangement of Eca.PRL2. These rearrangements are absent in the lampreys and likely have occurred after divergence of lamprey and gnathostome lineages, but prior to the 2Rjv. Conserved synteny (denoted by ~) is seen on Chr4, Chr16, Chr9, Chr12, Chr11, and Chr14 of Eca in comparisons with related chromosomes of Cmi and Gga.

at ~38 kDa and ~76 kDa were detected in extracts of Pma juvenile pituitary (Fig. 3*A*). In adult pituitary, a major ~40-kDa band was detected; immunostaining of all bands was diminished with preadsorbed antibody (Fig. 3*A*). Bands of similar size (40 and 76 kDa) also were detected in pituitary extracts of two female and four male adults (Fig. 3*B*).

Monoclonal HEK293 cells, stably expressing the gene encoding Pma.PRL-L with an N-terminal His-tag, secreted recombinant proteins. The HEK293-derived rPRL-L was collected from culture media with a His-tag affinity column and eluted with 50 mM and 100 mM of imidazole into two fractions, e1 and e2, respectively. Immunoblotting with Ab-lPRL detected a dense band at ~70 kDa in e1 and a 35-kDa band in e2 that diminished with preadsorbed Ab-lPRL (Fig. 3*C*).

The recombinant sea lamprey GH (rGH) produced by *E. coli* was ~22 kDa in immunoblotting with the antibody to lamprey GH (Ab-lGH), which is similar to the predicted size of the mature protein (Fig. 3*D*). A pituitary protein of similar size was detected in Pma adults (Fig. 3 *B* and *D*). The immunoreactive bands diminished in negative controls, using preadsorbed Ab-lGH (Fig. 3*D*). The Ab-lGH and Ab-lPRL had no cross-immunoreactivity with rPRL-L and rGH, respectively (Fig. 3 *A* and *D*).

Ligand-Receptor Binding Characteristics. Specific binding of ^{125}I–rPRL-L (*E. coli* derived) to membrane extracts of PRLR-HEK cells (~8%) was significantly greater ($P < 0.001$) than to extracts of GHR-HEK cells (~4%) or to extracts of nontransfected HEK cells (Fig. 3*E*). Competition studies revealed that Pma.PRLR preferentially bound to rPRL-L, as demonstrated by displacement of ^{125}I–rPRL-L from PRLR-HEK membrane extracts by low concentrations of rPRL-L (half maximal inhibitory concentration [IC_{50}], 37 nM; whereas rGH was a weak competitor of ^{125}I–rPRL-L (IC_{50}, ~294 nM (Fig. 3*F*). Pma.GHR preferentially bound rGH, as demonstrated by displacement of ^{125}I–rGH from GHR-HEK membrane extracts by low concentrations of rGH (IC_{50}, ~81 nM); whereas low concentrations of rPRL-L were ineffective in displacing ^{125}I–rGH (Fig. 3*G*).

Tissue Distribution of PRL-L and GH in Pma. PRL-L and GH mRNAs were detected predominately in the pituitary of juvenile Pma, with extremely low levels detected in the brain, whole blood cells, or other major peripheral tissues (Fig. 4*A*). Immunostaining of sagittal sections with Ab-lPRL and Ab-lGH was confined to the PPD; neither Ab-lPRL nor Ab-lGH immunostaining was observed in rostral pars distalis (RPD), pars intermedia, or hypothalamus of juveniles (Fig. 5 *A* and *C*). The immunostaining diminished in negative controls using preadsorbed antibodies (Fig. 5 *B* and *D*). In larvae, immunostaining with Ab-lPRL was very weak in the PPD (Fig. 5*E*), whereas strong staining with Ab-lGH was scattered in the PPD (Fig. 5*F*).

Abundance of PRL-L and GH mRNAs in Different Life-Cycle Stages of Pma. The abundance of PRL-L mRNA in the pituitary was significantly greater in adult Pma compared with larvae ($P = 0.008$; Fig. 4*B*). Similarly, the abundance of GH mRNA was greater in adults than levels found in either juveniles or in larvae ($P = 0.01$; Fig. 4*B*). Levels of GH mRNA were significantly greater than those of PRL-L in adults ($P < 0.001$).

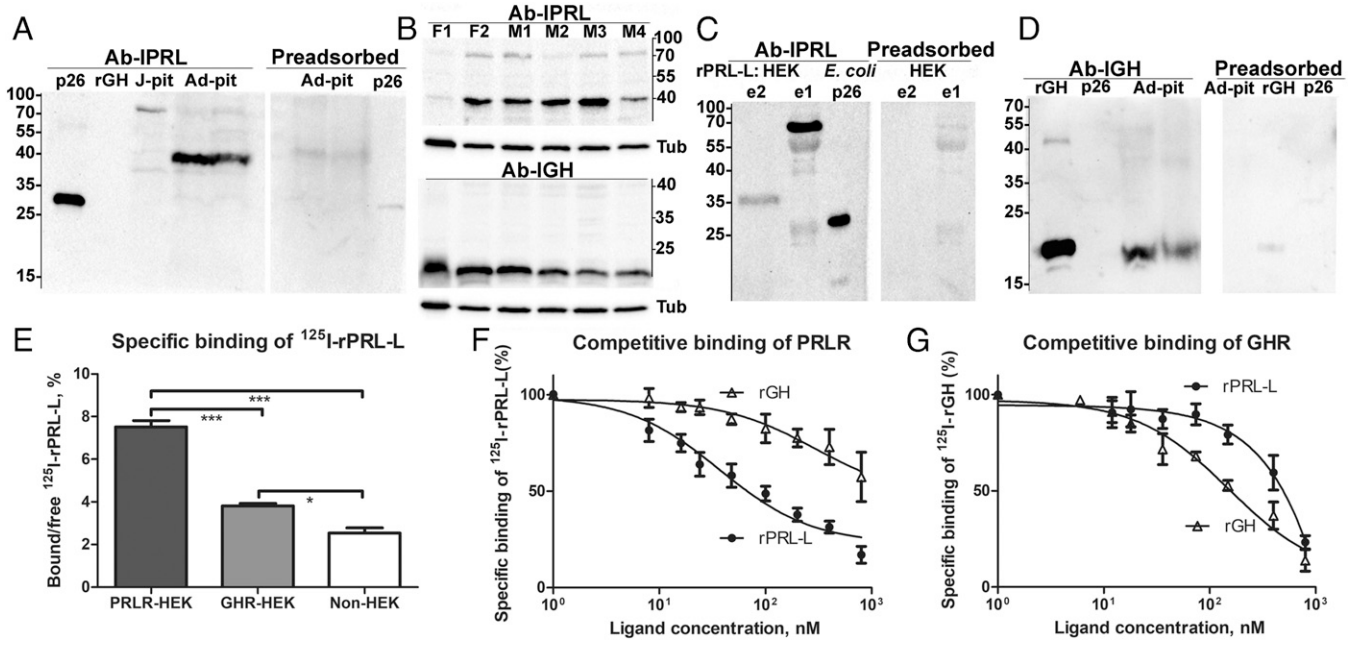

Fig. 3. Characterization of sea lamprey GH and PRL-L and ligand-receptor binding. (*A*–*C*) Immunoblotting with the antibody to lamprey PRL-L (Ab-lPRL) detected rPRL-L produced by *Escherichia coli* as a single band at ∼26 kDa (p26) as well as a faint band at ∼38 kDa and a denser band at ∼76 kDa in extracts from juvenile pituitary (J-pit) and a major band at ∼40 kDa in adult pituitary (Ad-pit). All bands diminished with preadsorbed antibody neutralized by antigen; Ab-lPRL was specific and did not detect rGH produced by *E. coli*. (*B*) A dense band at ∼40 kDa and a weak band at ∼76 kDa were detected by Ab-lPRL in pituitary extracts from two female (F) and four male (M) adults; β-tubulin (Tub) was used as reference protein. (*C*) Monoclonal HEK293 cells (HEK) produced two isoforms of PRL-L that were eluted to two fractions (e1 and e2) from His-tag affinity column, and immunoblotting detected a strong band at ∼70 kDa in e1 and a band at ∼35 kDa in e2; the bands diminished with preadsorbed antibody. (*B* and *D*) Immunoblotting with Ab-lGH detected a single band at ∼22 kDa in the pituitary of two females and four males (*B*) as well as a single band at ∼22 kDa for rGH and in Ad-pit (*D*). The bands diminished with preadsorbed antibody; the Ab-lGH was specific and did not detect rPRL-L (*D*). (*E*) Specific binding of ^{125}I–rPRL-L *(E. coli* derived) to membrane extracts of HEK293 cells individually expressing PRLR and GHR and of nontransfected HEK293 cells. (*F* and *G*) Displacement of ^{125}I–rPRL-L and ^{125}I–rGH binding to PRLR and GHR, respectively, by serial dilutions of rPRL-L and rGH. Specific binding is expressed as a percentage of total specific binding; data are reported as mean ± SE (n = 4 to 6). *$P < 0.05$; ***$P < 0.001$.

During metamorphosis of Pma, levels of PRL-L mRNA progressively increased, reaching peak levels at mid metamorphosis (stage 3) ($P < 0.0001$); thereafter, the abundance of PRL-L mRNA declined in the final stage of metamorphosis (stage 7) and in postmetamorphic juveniles to levels comparable with those at the initial stage of metamorphosis (Fig. 4*C*). By

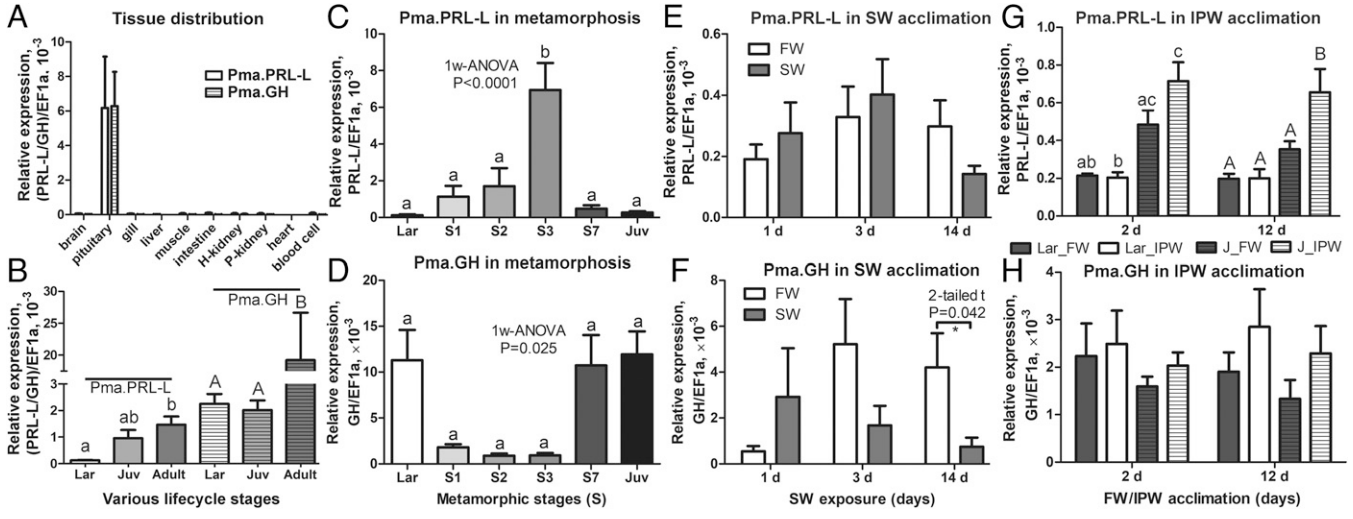

Fig. 4. Abundance of PRL-L and GH mRNAs in the pituitary of sea lamprey at different life-cycle stages and during acclimation to different environmental salinities. (*A*–*D*) Abundance of PRL-L and GH mRNAs in various tissues of juveniles (n = 3; *A*), at various life-cycle stages (*B*), including larvae (Lar; n = 6), juveniles (Juv; n = 7), and upstream migrating adults (n = 5), and in metamorphic transformers (*C* and *D*) at stage 1 (S1; n = 6), stage 2 (S2; n = 5), stage 3 (S3; n = 9), and stage 7 (S7; n = 11), compared with larvae (n = 18) and postmetamorphic juveniles (n = 16). Different letters denote significant differences among groups in one-way ANOVA with Turkey's post hoc test; $P < 0.05$ in one-way (1w) ANOVA (*C* and *D*). (*E* and *F*) Abundance of PRL-L and GH mRNAs in SW-acclimated (n = 9) and FW-acclimated juveniles (n = 6 to 9); two-tailed t test $P = 0.042$ in comparison of FW and SW groups at 14 d (n = 9), while in one-way ANOVA, $P > 0.05$. (*G* and *H*) Abundance of PRL-L and GH mRNAs in FW-acclimated larvae (solid bar; n = 9), IPW-acclimated larvae (open bar; n = 9), FW-acclimated juveniles (striped solid bar; n = 9), and IPW-acclimated juveniles (striped bar; n = 9) after 2 and 12 d. Abbreviations: H-kidney, head kidney; P-kidney, posterior kidney; J, juvenile. Different letters denote significant differences among groups in two-way ANOVA with Bonferroni's post hoc test. mRNA abundance was normalized to reference gene EF1a that had stable expression in each tissue or condition. Data are presented as mean ± SE.

contrast, the abundance of GH mRNA was initially high in larvae, then declined in early to mid metamorphic stages (stages 1 through 3); thereafter, levels of GH mRNA increased in the final stage of metamorphosis and in juveniles with large variation (Fig. 4*D*). Overall, there was a significant difference (one-way ANOVA, $P = 0.025$) in the abundance of pituitary GH mRNA among those groups (Fig. 4*D*).

Effects of Salinity on the Abundance of PRL-L and GH in Pma. Exposure of juvenile Pma to seawater (SW) did not significantly alter pituitary levels of PRL-L or GH mRNAs ($P = 0.22$ and $P = 0.16$, respectively; Fig. 4 *E* and *F*), except a significant difference in levels of GH mRNA was observed between FW and SW exposure for 14 d (*t* test, $P = 0.042$; Fig. 4*F*).

Acclimation of juveniles to ion-poor water (IPW) for 12 d increased the abundance of PRL-L mRNA in the pituitary compared with levels seen in FW controls ($P < 0.05$; Fig. 4*G*). The abundance of PRL-L mRNA in pituitaries of larvae was lower than that in IPW-acclimated juveniles at 2 d ($P < 0.0001$) and at 12 d ($P < 0.001$), and exposure of larvae to IPW did not affect the abundance of PRL-L mRNA ($P > 0.05$; Fig. 4*G*). Exposure to IPW had no effect on the abundance of Pma.GH mRNA in the pituitaries of larvae or juveniles ($P > 0.05$; Fig. 4*H*).

Immunostaining with Ab-lPRL in the PPD was similar in juveniles acclimated to FW or IPW for 2 d (Fig. 5 *G* and *H*); however, after 10 d, immunostaining was significantly greater in the PPD of IPW-acclimated juveniles compared with FW controls ($P < 0.001$; Fig. 5 *I*–*K*). Immunostaining with Ab-lGH appeared comparable in the PPD between the FW and IPW-acclimated juveniles (Fig. 5 *L* and *M*).

In Vivo Effects of PRL-L and GH on Juvenile Pma. Intraperitoneal administration of *E. coli*–produced rGH and rPRL-L to FW-acclimated juveniles for 2 d significantly reduced levels of GHR and PRLR mRNAs in the liver and gill ($P < 0.001$; Fig. 6 *A*, *B*, *D*, and *E*). Levels of IGF mRNA also were significantly reduced by both rGH ($P < 0.05$) and rPRL-L ($P < 0.001$) after 2 d in FW (Fig. 6*C*). By contrast, mRNA levels of suppressor of cytokine signaling 3 (SOCS3), known to suppress cytokine signaling, which were initially low, were significantly elevated in gill ($P < 0.001$; Fig. 6*F*) and liver ($P < 0.001$; *SI Appendix*, Fig. S4*A*) by rGH and rPRL-L treatment after 2 d. In general, levels of GHR, PRLR, IGF, and SOCS3 mRNAs were similar between the FW and SW control groups. Alterations in the mRNA levels of hepatic and branchial GHR, hepatic and branchial PRLR, hepatic and branchial SOCS3, and hepatic IGF induced by rGH and rPRL-L following 2 d in FW were not observed after hormone treatments for 5 d in combination with SW exposure (Fig. 6 *A*–*F* and *SI Appendix*, Fig. S4*A*).

Exposure of juveniles to SW altered the mRNA expression of several key ion transporters critical for osmoregulation. Notably, the branchial abundance of ATP1B2 and SLC12A3.3 mRNAs (*t* test, $P = 0.02$ and $P = 0.03$, respectively; Fig. 6 *H* and *I*) decreased after 2 d in SW, whereas branchial abundance of ATP1B3 and SLC12A2.2 mRNAs significantly increased after 2 d in SW (*t* test, $P = 0.002$ and $P = 0.05$, respectively; Fig. 6 *J* and *K*). Although mRNA levels of ATP1A1 in gill tended to decline after SW exposure, the effect was not significant (*t* test, $P = 0.17$; Fig. 6*G*). SW challenge experiments confirmed these effects on branchial ion transporters. Levels of ATP1A1 ($P < 0.0001$), ATP1B2 ($P < 0.0001$), and SLC12A3.3 ($P < 0.0001$) mRNAs were significantly reduced following 1, 3, and 14 d of SW exposure compared with levels observed in FW (*SI Appendix*, Table S1). By contrast, ATP1B3 ($P = 0.0003$) and SLC12A2.2 ($P = 0.042$) mRNA levels were significantly higher than those observed in FW (*SI Appendix*, Table S1). Levels of SLC12A2.1 were not affected by SW exposure (Fig. 6*L* and *SI Appendix*, Table S1).

Treatment with rPRL-L blocked the SW-associated inhibition of the FW-adapting ion transporters (ATP1A1, ATP1B2,

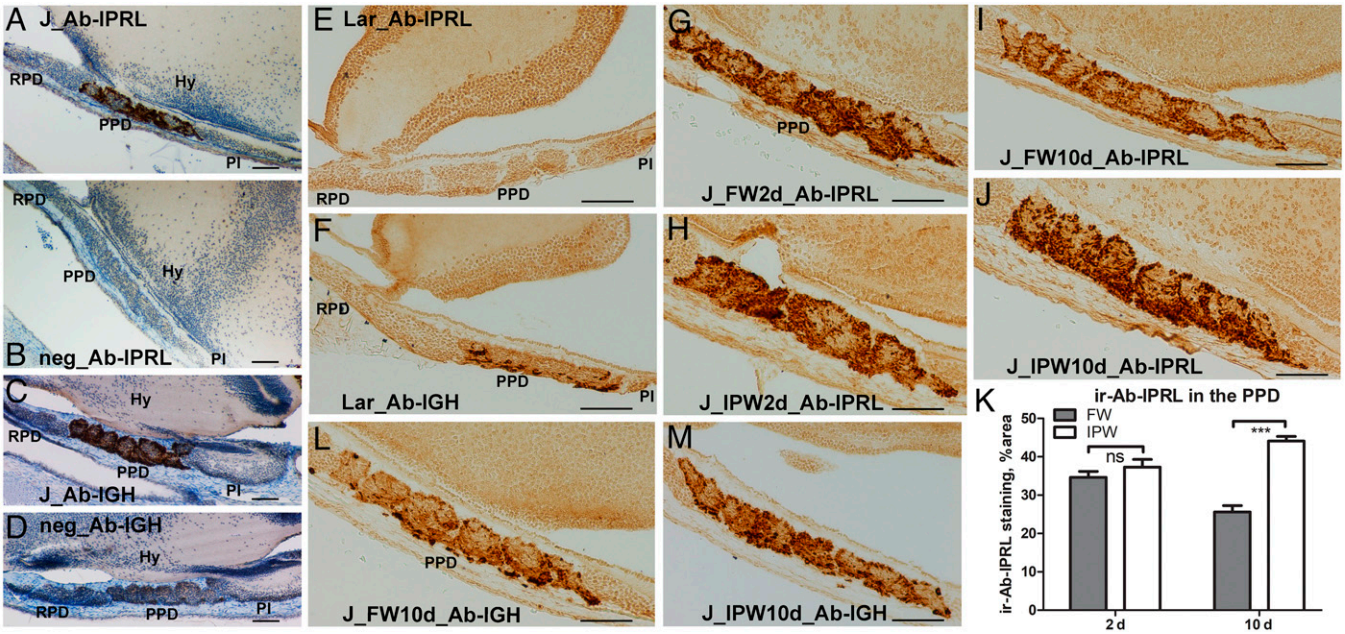

Fig. 5. Immunostaining of PRL-L and GH in the pituitary of sea lamprey. (*A*–*D*) On sagittal sections, immunoreactive (ir) staining with Ab-lPRL (*A*) and Ab-lGH (*C*) appeared in the PPD but was negligible in the RPD, pars intermedia (PI), or hypothalamus (Hy). The immunostaining diminished with preadsorbed antibodies (negative controls; *B* and *D*). Cell nuclei stained by hematoxylin. (*E*) Ir staining of PRL-L was very weak in the PPD of larvae (lar). (*F*) Ir-GH staining was scattered throughout PPD of larvae. (*G*–*J*) Ir–PRL-L staining in the PPD of juveniles (J) acclimated to FW (*G*) ($n = 3$) and IPW (*H*) ($n = 3$) for 2 d (2d) or for 10 d (10d) (*I*) in FW ($n = 3$) and in IPW (*J*) ($n = 3$). (*K*) Semiquantification of ir–PRL-L staining, percent area of the PPD (30 to 40 images per group) showed a significant difference between FW and IPW juveniles after 10 d. Data presented as mean ± SE. ***$P < 0.001$. ns, nonsignificant. (*L* and *M*) Ir-GH staining in the PPD of FW- and IPW-acclimated juveniles after 10 d, respectively. Scale bars, 100 μm.

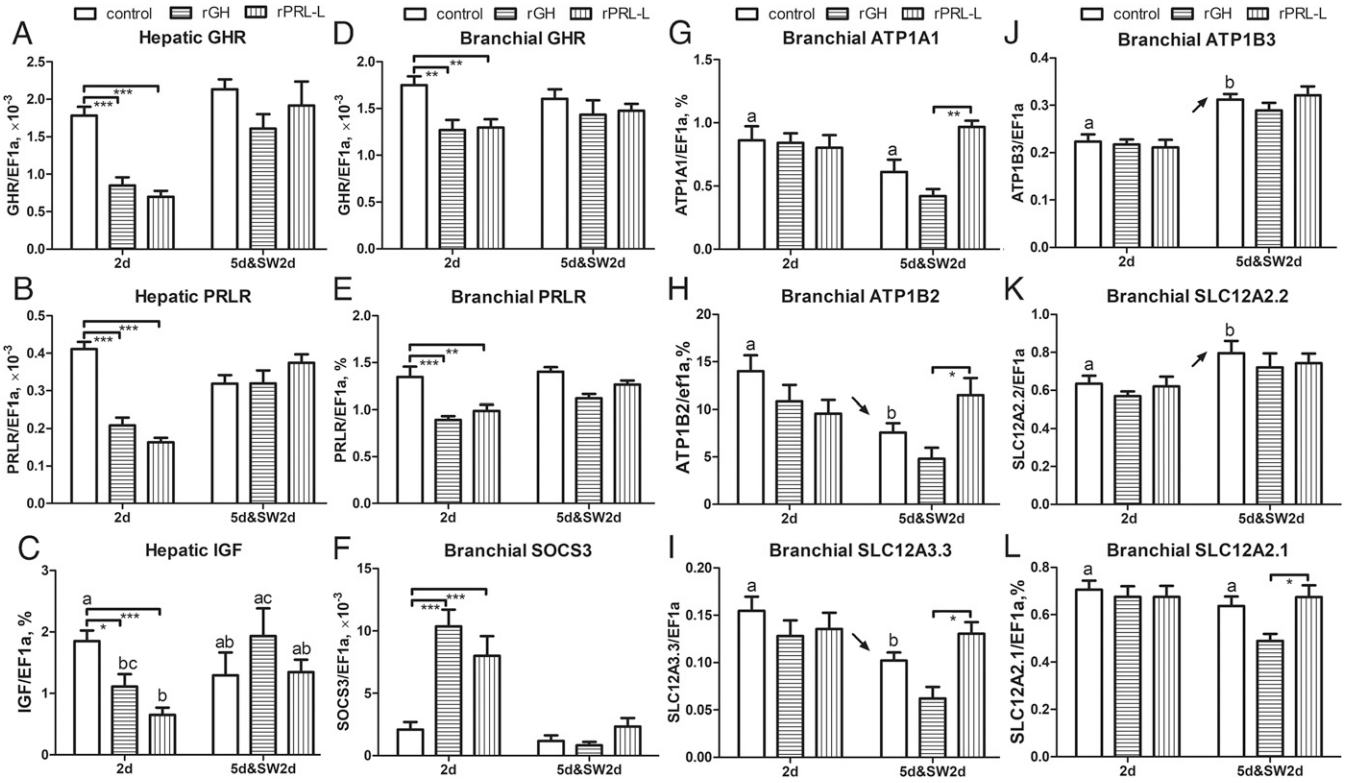

Fig. 6. Effects of recombinant GH and PRL-L and of exposure to SW on the abundance of mRNAs encoding receptors, signaling elements, and ion transporters in the liver and gill of juvenile sea lampreys. Juveniles acclimated to FW were injected with a single dose of rGH, rPRL-L, or saline, transferred to SW 3 d after injection, and acclimated in SW for 2 d. Liver and gill tissues were sampled 2 d (2d; $n = 10$) and 5 d (5d&SW2d; $n = 6$) after the injection. (*A–C*) Effects on abundance of mRNAs encoding hepatic GHR (*A*), PRLR (*B*), and IGF (*C*). (*D–F*) Effects on abundance of mRNAs encoding branchial GHR (*D*), PRLR (*E*), and SOCS3 (*F*). (*G–L*) Effects of hormones and SW exposure on abundance of mRNAs encoding selected ion transporters in gill, including ATPase subunit α1 (ATP1A1; *G*), subunits β2 and β3 (ATP1B2, ATP1B3; *H* and *J*), a SLC12A3 variant (SLC12A3.3; *I*), and two variants of SLC12A2 (*K* and *L*). mRNA abundance was normalized to EF1a. All data are presented as mean ± SE; brackets and/or different letters denote significant differences between groups. $*P < 0.05$; $**P < 0.01$; $***P < 0.001$. Arrows depict stimulatory or inhibitory effects of SW exposure (comparing FW control group and SW control group; $P < 0.05$).

and SLC12A3.3), and levels of these mRNAs were significantly higher than those in the rGH-injected group exposed to SW ($P < 0.01$, $P < 0.05$, and $P < 0.05$, respectively; Fig. 6 *G–I*). Neither rGH nor rPRL-L affected the SW-associated stimulation of the SW-adapting ion transporters (i.e., ATP1B3, SLC12A2.2) (Fig. 6 *J* and *K*). Notably, neither hormone treatment affected mRNA expression for any ion transporter in FW-acclimated juveniles 2 d after injection (Fig. 6 *G–L*).

Discussion

In this study, we identified a second member of the GH/PRL gene family in the pituitary of Pma, the addition of which provides important insight into the early evolution of the gene family. Structural, phylogenetic, and syntenic analyses, together with functional data, support the identification of this hormone as PRL-L. With the completion of other lamprey genomes, so far, we identified PRL-L orthologs in Pma, Arctic lamprey, and Far Eastern brook lamprey (*SI Appendix*, Figs. S1 and S5). The presence of PRL-L in the other major group of agnathans, hagfish, remains unclear, as we only were able to identify a partial sequence of a GH-like gene in the incomplete genome dataset (*SI Appendix*, Fig. S5).

Similarities in the gene and protein structures indicate that the Pma.GH and Pma.PRL-L are structurally related to the GH/PRL family. The lamprey PRL-L gene was not previously annotated in the genomes, likely due to low identity in amino acid sequences (≤29%) and codon usage bias and higher frequencies for GC-rich codons, common characteristics of lamprey genes (29, 30). As a result, node support for lamprey PRL-L in the phylogeny was very weak. Addition of the lamprey PRL-L to the phylogeny changed the tree topology compared with previous phylogenies of the GH/PRL gene family (1, 12) that clustered lamprey GH directly at the base of gnathostome GH with good node support. Nevertheless, the current phylogeny supports the relationship of lamprey GH and PRL-L with the gnathostome GH/PRL family, but with uncertainty of the timing of divergence, due to lack of an outgroup. The amphioxus GH-like proteins are highly derived (*SI Appendix*, Fig. S5) and are not a reliable outgroup for the phylogeny, which also was indicated in a previous study (1). The partial sequence annotated as hagfish GH-like also was excluded in the phylogeny because protein alignment and modeling indicated that the predicted gene sequence is likely only partially correct (*SI Appendix*, Fig. S5). It also should be noted that the four conserved Cys residues that form two disulfide bonds in gnathostome GHs and PRLs (1, 13) also are conserved in Pma.GH and Pma.PRL-L, a pattern that is absent in the amphioxus GH-like proteins (*SI Appendix*, Figs. S1 and S5), indicating that the two disulfide bonds may have emerged in ancestral vertebrates.

The identification of the paralogs of the neighboring genes that are present in the lamprey and jawed vertebrates or only in jawed vertebrates suggests separate gene duplication events, which likely correspond to the 1R whole-genome duplication shared by all extant vertebrates and the 2R genome duplication in 2Rjv (14, 16). The synteny analysis of the neighboring gene families reveals chromosomal rearrangements that may have occurred in the speciation of gnathostome progenitors prior to 2Rjv (14, 16). The rearranged loci of the various GH/PRL

family members and their neighboring genes are largely conserved in jawed vertebrates, as shown in the present study as well as in previous studies (1, 13). None of the duplicates of SL, PRL, or PRL2 appear to be preserved after 2Rjv, likely due to asymmetrical gene loss (14), and chromosomal rearrangements of GH and/or PRL2 likely occurred in some species. Loss of SL occurred in amniotes and some amphibian species, and the loss of PRL2 occurred in amphibians and mammals (1). Nevertheless, the synteny analysis supports the notion that the four members of the GH/PRL family emerged prior to 2Rjv. This also is suggested in the scenarios for the evolution of the GH/PRL family proposed by Ocampo Daza and Larhammar (1).

The discovery of lamprey PRL-L advances the understanding of gene expansion of the GH/PRL gene family in the 1R and 2Rjv. Based on the finding of paralogs, GH-bearing Pma.Chr3 and Pma.Chr37 are likely two descendants after the 1R, while the PRL-L–bearing Pma.Chr62 is related to Pma.Chr32. A plausible scenario (Fig. 7) is that Pma.GH is retained on the Pma.Chr3 after the 1R, while its duplicate was not found and may have been lost in the lamprey. The descendants were preserved as GH and SL in the stem lineages leading to jawed vertebrates, but their loci may have been exchanged on the paralogous chromosomes (Fig. 7). Correspondingly, GH was retained on Chr14 in Eca, with the gene families that are syntenic on lamprey Chr37. Chromosomal rearrangements prior to 2Rjv, perhaps including fusion and mixing events (14), may have rearranged the loci of those gene families that were initially neighboring SL and PRL (Fig. 7), leading to the mixing patterns of the neighboring genes on the SL- and PRL-bearing chromosomes in jawed vertebrates.

The presence of paralogs suggests that the PRL-L–bearing Chr62 is related to Chr32 in sea lamprey. The paralogy group on Pma.Chr32 is identified on the PRL2-bearing Chr1 of Gga and Chr4 of Eca, on which nearly half of the gene families in the vicinity of Pma.PRL-L also are located. The rest of the gene families are mostly located on the SL-bearing chromosome or the syntenic chromosome, and a few are retained on the PRL-bearing or related chromosome. A plausible scenario (Fig. 7) is that PRL2 and PRL were both conserved after 1R in the stem lineages leading to jawed vertebrates, whereas PRL-L was retained in lampreys, and the other duplicate was not found and may have been lost. Half of the gene families in the vicinity of Pma.PRL-L were located on the ancestral PRL2-bearing chromosome (prior to PRL2 rearrangement) in the gnathostome stem lineages, while the rest were initially retained in the vicinity of PRL but further rearranged to the SL-bearing chromosome by chromosomal rearrangements prior to 2Rjv.

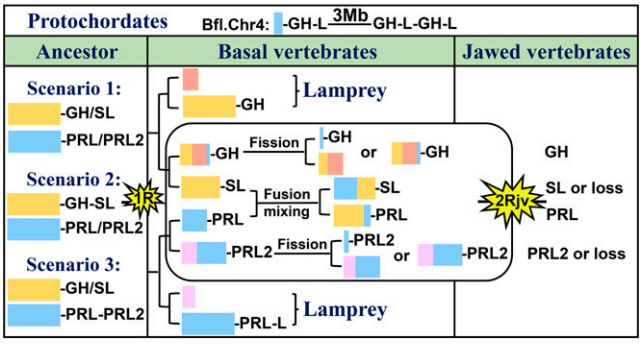

Fig. 7. Model of early evolution of the GH/PRL gene family in vertebrates. The syntenic blocks in blue contain the 31 gene families in the vicinity of Pma.PRL-L in the early vertebrate ancestor. The syntenic blocks in yellow contain the 29 gene families in the vicinity of Pma.GH. The blocks in other colors depict the paralogs from those gene families that arose in 1R whole-genome duplication, but prior to 2Rjv. The block length is proportional to the rate of the representatives from those gene families that are retained on the same chromosome. The calculation is based on the chromosomal comparisons of sea lamprey with Eca, Cmi, and Gga. Three GH-L genes are located on Chr4 in Florida lancelet (Bfl). The ancestral GH/SL and PRL/PRL2 diverged prior to the 1R, but the present study cannot exclude the scenario of adjacent GH and SL (GH-SL) or adjacent PRL and PRL2 (PRL-PRL2). The 1R event likely gave rise to four descendants in the basal vertebrates, which are conserved as GH, SL, PRL, and PRL2 in the stem lineages leading to jawed vertebrates; GH and PRL-L are extant in the lamprey. Chromosomal rearrangements, including fusion, mixing, and fission, may have occurred prior to the 2Rjv event and caused rearrangements of GH, SL, PRL, and PRL2. Further loss of SL and/or PRL2 occurred in a wide variety of jawed vertebrates.

In protochordates, three GH-like genes are located on Bfl.Chr4 in Florida lancelet (*SI Appendix*, Fig. S6). It is unclear whether they arose prior to vertebrates or independently by local gene duplication. Our synteny analysis suggests at least two ancestors existed prior to 1R: GH/SL and PRL/PRL2; however, we cannot exclude the possibility of adjacent GH and SL (GH-SL) or adjacent PRL and PRL2 (PRL-PRL2) on the ancestral chromosome (Fig. 7).

Identification of pituitary Pma.PRL-L by immunoblotting revealed proteins larger in size than the predicted 26 kDa, as well as an apparent dimer of >70 kDa. Specificity in the detection of these proteins was demonstrated by antibody preadsorption. Small differences were seen in the sizes of pituitary Pma.PRL-L in juvenile (38 kDa) and in adult (40 kDa) and rPRL-L (35 kDa) generated by HEK293 cells. Posttranslational modifications of Pma.PRL-L may occur at potential sites of Ser, Thr, or Tyr phosphorylation and at Thr^{211} residue of O-glycosylation (*SI Appendix*, Fig. S7). Posttranslational modification of PRL, including dimerization, polymerization, phosphorylation, glycosylation, sulfation, and deamidation, has been reported in a wide range of species, and the degree of modification is physiologically relevant (3, 31). For example, the posttranslational modifications of PRL can result in high-molecular-weight forms and alter hormone activity by adjusting receptor binding, hormone secretion, and metabolic clearance (3). The immunoreactive band of ~76 kDa appeared to be a dimerized isoform of Pma.PRL-L, which was not dissociated in standard sodium dodecyl sulfate–polyacrylamide gel electrophoresis under reducing conditions. This may be similar to nondissociable GH dimers (minor form, 1%) observed in the human pituitary (32), which are characterized as interchain disulfide–linked homodimers and are exceptionally resistant to reducing agents (33). Further study is needed to clarify the extent and types of posttranslational modifications of Pma.PRL-L. By contrast, monomeric Pma.GH is similar in size to that of the predicted protein and exists as the major form in the pituitary. This is similar to monomeric mammalian GH, which constitutes ~60% of the isoforms in the pituitary (4, 32).

In a previous study, two putative receptors were identified in sea lamprey as the orthologs to gnathostome GHR and PRLR, respectively (26). In this study, the sea lamprey GHR and PRLR stably expressed in HEK cells revealed distinct but overlapping binding characteristics. PRLR preferentially bound to rPRL-L, whereas GHR preferentially bound to rGH, although there was a low level of cross-binding observed. Notably, both hormones down-regulated the expression of both receptors, as seen after 2 d of in vivo hormone treatment. Down-regulation of GHR and PRLR mRNA expression concomitant with increased levels of SOCS3 mRNA indicates a negative feedback regulation of hormone signaling. SOCS3 is an inhibitor of cytokine signaling in the cascade of Janus kinase (JAK) and a signal transducer and activator of transcription (STAT) (34). Although the JAK-STAT

signaling cascade is largely unknown in jawless vertebrates, JAK2 and STAT proteins are present in the sea lamprey genome, and the lamprey GHR and PRLR have potential docking sites for phosphorylation of JAK and STAT (26). Thus, the classic JAK2-STAT(3/5) cascades (3, 4) likely mediates cytokine signaling in the lamprey. The extent to which adjusting receptor abundance and/or linkage(s) to cell-signaling cascades regulate the biological activities of GH and PRL-L in sea lamprey remains to be examined.

The major site for producing Pma.PRL-L and Pma.GH is the pituitary gland, which is similar to the pattern of distribution for PRL, GH, and SL in jawed vertebrates (2). Immunostaining with Ab-lPRL indicates that Pma.PRL-L is predominately distributed in the PPD, similar to that of Pma.GH (12, 23). This pattern is somewhat different to what is observed for jawed vertebrates. For example, in teleost fishes, somatotrophs and lactotrophs are distributed in the PPD and RPD, respectively (2, 35), while SL is produced in the PI (36). PRL2 is located in extrapituitary tissues, such as eye and brain, in zebrafish (5, 37), and in brain and some peripheral tissues in Gga (5). Based on tissue distribution, the pattern of lamprey PRL-L expression is more like that of PRL than that of extrapituitary PRL2.

A progressive up-regulation in the abundance of pituitary Pma.PRL-L mRNA was seen in the early stages of metamorphosis, especially at stage 3, whereas Pma.GH mRNA levels were suppressed at the early stages, corresponding to its low protein abundance that was previously measured in the metamorphic transformers (23, 24). *Geotria* lamprey transformers in which PPD was surgically removed were unable to proceed through metamorphosis beyond stage 3 (25). We previously observed an increase of branchial PRLR mRNA abundance beyond stage 5, concomitant with acquisition of SW tolerance (26), indicating involvement of PRL-L signaling in the gill development. Collectively, these findings indicate that PPD-derived PRL-L could be involved in regulating metamorphosis of sea lamprey. Further study should be performed to determine if there are direct action(s) of Pma.PRL-L in organ development or other processes during lamprey metamorphosis.

Hepatic IGF mRNA expression was not stimulated by in vivo rGH treatment of juvenile sea lamprey. This result is in contrast to the results of Kawauchi et al. (12), who found pituitary GH extract stimulated hepatic IGF mRNA expression in adult lamprey in vitro. This difference may be explained by several factors. First, in the present study, hepatic IGF mRNA levels were suppressed in animals that were treated with rGH or rPRL-L for 2 d, a period during which expression of GHR and PRLR mRNAs was down-regulated and SOCS3 mRNA expression was up-regulated. Together, these changes would have reduced sensitivity to rGH and rPRL-L and deactivated the cell-signaling cascades (4, 34), leading to reduced IGF expression. This notion is supported by the observation that the suppressive effects of rGH or rPRL-L on IGF mRNA levels were no longer observed when the abundance of GHR, PRLR, and SOCS3 mRNAs returned to normal levels after 5 d and in combination with SW exposure. Second, the developmental stage was different (adults versus juveniles), and the juveniles in this study did not feed, a natural condition that occurs after completion of metamorphosis until parasitism in the ocean begins. Nutrients are crucial regulators of the GH/IGF-I axis to promote growth under sufficient energy conditions (4, 38). Acquired GH resistance concomitant with elevated GH and depressed IGF-I levels is characterized in teleosts as a strategy for coping with long-term fasting (39, 40). Furthermore, positive nutrient status (i.e., feeding) has been shown in teleosts to be required for GH to stimulate IGF-I production/release (41). It is reasonable to suggest that commencement of feeding may be a prerequisite for GH stimulation of IGF in the lamprey. This hypothesis is supported by the elevated levels of Pma.GH in adults, corresponding to the increased numbers of somatotrophs in parasitic and adult lamprey (23, 24).

Acclimation to changes in environmental salinity relies on the presence of ion transporters in the gill and other osmoregulatory tissues as seen in euryhaline teleosts (42). Many of these same ion transporters increase in abundance during metamorphosis when sea lampreys develop SW tolerance (43). In this study, we found that the mRNA expression of six ion transporters responded differentially to SW acclimation of sea lamprey. A Na^+/K^+-ATPase was previously characterized in sea lamprey as an SW-stimulated ion pump (44, 45). In this study, we identified two variants of Na^+/K^+-ATPase subunit β, including ATP1B3, the mRNA expression of which was stimulated by SW, and ATP1B2, the mRNA expression of which was inhibited by SW. mRNA expression of the SW-inhibited ATP1B2 was significantly correlated with that of the subunit α1, ATP1A1 ($P < 0.0001$; *SI Appendix*, Fig. S4*B*), the mRNA expression of which also was inhibited by SW; thus, the two subunits may constitute an FW-adaptive Na^+/K^+-ATPase for ion absorption. Another FW-adaptive ion transporter is SLC12A3.3, which is similar to a previously characterized sea lamprey SLC12A3 that was activated in FW (46). Another SW-stimulated ion transporter identified in the present study is SLC12A2.2, which is similar to an SLC12A2 that was activated in SW in previous studies (44), while the apically located SLC12A2.1 was generally not affected by SW (44).

The role of PRL-L in osmoregulation of sea lamprey is supported by two lines of evidence. First, transfer of juvenile sea lamprey to IPW (a hypoosmotic environment) increased the abundance of pituitary PRL-L mRNA, compared with the FW-acclimated juveniles and larvae. Notably, long-term exposure to IPW (10 d) significantly increased immunoreactive PRL-L in the PPD of juveniles. Second, treatment of juveniles with rPRL-L blocked the SW-associated decrease in expression of SLC12A3.3 and the putative FW-adapting Na^+/K^+-ATPase (composed of two subunits, ATP1A1 and ATP1B2), which are essential for absorption of Na^+, K^+, and Cl^- (46), but had no effect on the SW-associated increase in expression of an SW-adapting Na^+/K^+-ATPase composed of ATP1B3 (subunit β3) and SLC12A2.2 that function in salt secretion in SW (44). Taken together, these observations indicate that PRL-L plays a role in osmotic regulation of sea lamprey by, at least partially, regulating FW-adapting ion transporters for ion uptake and homeostasis of Na^+, K^+, and Cl^-, which is similar to the role of PRLs in teleosts (27, 47).

Conclusion. We discovered a PRL-L in sea lamprey, establishing the existence of two members of the GH/PRL family in agnathans. Conservation in gene and protein structures, phylogeny, and synteny indicates that lamprey PRL-L is an ortholog of gnathostome PRL/PRL2. A model was proposed for the evolution of the GH/PRL family in early vertebrates (Fig. 7), in which at least two ancestral genes likely were present prior to the 1R duplication event, and that four members of the gene family likely emerged prior to the 2Rjv. In sea lamprey, both PRL-L and GH are produced primarily in the PPD of the pituitary and bind to their cognate receptor with high affinity. Pituitary PRL-L mRNA levels were very low in larvae but dramatically increased during metamorphosis at stage 3. Sea lamprey PRL-L mRNA and protein levels in the pituitary of juveniles were

stimulated by acclimation to hypoosmotic conditions. In vivo treatment with rPRL-L blocked SW-associated inhibition of FW-adapting ion transporters (an ATPase and SLC12A3). These findings reveal a function of PRL-L in osmoregulation of sea lamprey that is conserved for PRLs in jawed vertebrates.

Materials and Methods

Identification of the PRL-L Gene in Sea Lamprey. A short genomic sequence with similarity to GH and PRL was identified in sea lamprey genome Pmar_germline 1.0 (GenBank no. GCA002833325.1). This gene fragment was amplified by RT-PCR using pituitary cDNA as a template, and the absent 5′ sequence from the genome was obtained by 5′ rapid amplification of cDNA ends PCR. The full-length cDNA of Pma.PRL-L was obtained by PCR and included a partial 5′ untranslated region (UTR), a sequence encoding 255 amino acids, and a partial 3′-UTR (*SI Appendix*, Fig. S8). Information about primers is listed in *SI Appendix*, Table S2. The cDNA sequence, except the 5′-UTR and the sequence encoding the first 3 amino acids, was identified in an unplaced genomic scaffold (no. NW022639444.1) in sea lamprey genome kPetMar1 (no. GCA_010993595.1). Partial sequences, including the exons 1, 5, and 6, were identified on Chr62 (no. NC_046130.1) at the loci of 6.747, 6.766, and 6.769 Mb, respectively, while the sequence of exon 2 is likely incorrectly assembled at 5.926 Mb, but the exons 3 and 4 are absent on the Chr62, likely due to sequencing gap.

Searching for Orthologs in Agnathans. The amino acid sequence of Pma.PRL-L was searched by TBLASTN against the available genome datasets of agnathans (by February 2022). Exons 2 through 6 of a PRL-L ortholog are located on 2.03 to 2.05 Mb of Chr62 in the Far Eastern brook lamprey genome ASM1570882v1 (no. GCA_015708825.1) encoding 250 amino acids with 85% identity to Pma.PRL-L (*SI Appendix*, Fig. S5). Partial sequence of a PRL-L gene encoding 210 amino acids is identified on Scaffold84 in Arctic lamprey genome IMCB_Ljap_1.0 (no. GCA_018977245.1), while several fragments encoding around 40 amino acids are missing in exons 1 through 3 (*SI Appendix*, Fig. S5), likely due to the gaps.

The lamprey GH orthologs are located on Chr3 in sea lamprey genome kPetMar1, on scaffold5 in Arctic lamprey genome IMCB_Ljap_1.0, and on Chr26 in Far Eastern brook lamprey genome ASM1570882v1 (*SI Appendix*, Fig. S5). A partial GH-like gene including two exons (Ensembl no. ENSEBUG00000006986.1) was identified in inshore hagfish genome Eburgeri_3.2 (no. GCA_900186335.2). Protein modeling of the hagfish GH-like using human PRL (3d48.1.A) as template predicts protein composed of single helix with a C-terminal tail (*SI Appendix*, Fig. S5).

Phylogenetic and Synteny Analyses. Sequences of mature proteins (*SI Appendix*, Table S3) were aligned by the MUSCLE algorithm applied through AliView (48) software with default settings, and phylogenetic analysis was performed using the likelihood-based phylogenetic maximum likelihood method through SeaView 4.7 (49).

Thirty-one gene families neighboring Pma.PRL-L (*SI Appendix*, Table S4), located at 2.12 to 7.62 Mb on Pma.Chr62, were selected for synteny analysis; paralogs were found on Pma.Chr32 (*SI Appendix*, Table S5). Thirty of these gene families also were identified on Lre.Chr62 in Far Eastern brook lamprey (*SI Appendix*, Fig. S6). Moreover, 29 gene families neighboring Pma.GH at 20.30 to 23.79 Mb on Pma.Chr3 (*SI Appendix*, Table S6) were taken for analysis and also were identified on Lre.Chr26 of Far Eastern brook lamprey (*SI Appendix*, Fig. S6), and paralogs were found on Pma.Chr37 (*SI Appendix*, Table S7). Representatives from the repertoires of those gene families were identified in Eca (*SI Appendix*, Tables S8 and S9), Cmi (*SI Appendix*, Tables S10 and S11), and Gga (*SI Appendix*, Tables S12 and S13). These gnathostome species were selected because they underwent fewer large-scale genome rearrangements (1, 15, 16, 50).

Paralogs were defined in the Ensembl Genome Browser and classified into the following three groups based on their positions in the respective gene trees (*SI Appendix*, Tables S8 and S9): 1) ancient paralogs that diverged prior to vertebrates cluster in the clades rooted by *Ciona*, *Caenorhabditis*, or *Drosophila*; 2) paralogs that were found in lamprey/hagfish and jawed vertebrates cluster in the clades rooted by lamprey and/or hagfish; 3) paralogs that arose after divergence of lamprey and gnathostome lineages, cluster in the clades rooted by Cmi and/or Eca, and these paralogs were further queried for TBLASTN search against the lamprey genomes to confirm their emergences in jawed vertebrates.

Animal Experiments. Animal experiments were conducted at the US Geological Survey (USGS) Conte Anadromous Fish Research Laboratory, approved by USGS (protocol LB00A3O-117) and the University of Massachusetts (protocol no. 2016–0009) Institutional Animal Care and Use Committees.

Sea lamprey at various life stages were captured from the Connecticut River (MA, USA). In the SW experiment, juveniles were transferred to artificial SW (35 ppt). In the IPW experiment, larvae and juveniles were transferred to deionized water filtered through double deionization columns. For the in vivo hormone treatment study, FW-acclimated juveniles were injected with saline (control), rGH, or rPRL-L in saline solution at a single dose (5 μg protein/g of fish in 20 μL/g of fish volume). The dose for the single injection was selected based on previous experiments using GH/PRL (5 to 10 μg g^{-1} body weight) in teleosts that resulted in physiologic responses (51, 52).

Other Experiments. All experimental procedures are standard, including production of recombinant proteins and antibodies, immunoblotting, immunohistochemistry, radioactive iodine (^{125}I)-labeled ligand-receptor binding assay, cell transfection and generation of stable cell lines, and real-time qPCR. The details are described in *SI Appendix*.

Statistical Analysis. Kolmogorov-Smirnov tests were used to determine normality distribution of the treatment groups, and Levene's median test or F test were used to determine equality of variances. One-way ANOVA followed by a Tukey post hoc test was applied for comparisons at various stages of life cycle and metamorphosis. Two-way ANOVA followed by a Bonferroni's multiple comparisons test were applied for analysis in the studies of SW acclimation, IPW acclimation, and in vivo hormone treatments. Unpaired *t* test with two-tailed *P* values was used for comparison of two groups at the same time and for comparison of the saline-injected FW control and SW control in the in vivo treatment. Statistical analyses were made with GraphPad Prism 9. Differences were considered significant at $P < 0.05$, $P < 0.01$, and $P < 0.001$.

Data, Materials, and Software Availability. Raw data have been deposited in Dryad (10.5061/dryad.jdfn2z3dr) (53).

ACKNOWLEDGMENTS. This work was supported by the NSF (Grant 1558037 to M.A.S. and S.D.M.) We thank Dr. Dan Larhammar (Uppsala University, Sweden) for assistance with bioinformatics; Dr. James Carr (Texas Tech University, United States) for assistance with immunohistochemistry and ligand-receptor binding assay; Dr. Peter Keyel (Texas Tech University) for assistance with cell culture; and Amy M. Regish, Daniel Hall, and Dr. Ciaran A. Shaughnessy (US Geological Survey Conte Anadromous Fish Research Center) for assistance with animal collection and tissue sampling. We also thank Dr. Dan Larhammar and Dr. Jason Breves (Skidmore College) for critical evaluation of the manuscript. Any use of trade, product, or firm names is for descriptive purposes only and does not imply endorsement by the US Government.

1. D. Ocampo Daza, D. Larhammar, Evolution of the growth hormone, prolactin, prolactin 2 and somatolactin family. *Gen. Comp. Endocrinol.* **264**, 94–112 (2018).
2. D. O. Norris, J. A. Carr, "The hypothalamus-pituitary system in nonmammalian vertebrates" in *Vertebrate Endocrinology*, ed. 6 (Elsevier, 2020), pp. 151–204.
3. M. E. Freeman, B. Kanyicska, A. Lerant, G. Nagy, Prolactin: Structure, function, and regulation of secretion. *Physiol. Rev.* **80**, 1523–1631 (2000).
4. M. Caputo *et al.*, Regulation of GH and GH signaling by nutrients. *Cells* **10**, 1376 (2021).
5. Y. Wang, J. Li, A. H. Yan Kwok, W. Ge, F. C. Leung, A novel prolactin-like protein (PRL-L) gene in chickens and zebrafish: Cloning and characterization of its tissue expression. *Gen. Comp. Endocrinol.* **166**, 200–210 (2010).
6. G. Bu, X. Liang, J. Li, Y. Wang, Extra-pituitary prolactin (PRL) and prolactin-like protein (PRL-L) in chickens and zebrafish. *Gen. Comp. Endocrinol.* **220**, 143–153 (2015).
7. M. Ono *et al.*, cDNA cloning of somatolactin, a pituitary protein related to growth hormone and prolactin. *Proc. Natl. Acad. Sci. U.S.A.* **87**, 4330–4334 (1990).
8. M. O. Huising, C. P. Kruiswijk, G. Flik, Phylogeny and evolution of class-I helical cytokines. *J. Endocrinol.* **189**, 1–25 (2006).
9. S. Ouyang, F. He, Phylogeny of a growth hormone-like cytokine superfamily based upon 3D structure. *J. Mol. Evol.* **56**, 131–136 (2003).
10. M. Li, Z. Gao, D. Ji, S. Zhang, Functional characterization of GH-like homolog in amphioxus reveals an ancient origin of GH/GH receptor system. *Endocrinology* **155**, 4818–4830 (2014).

11. M. Nozaki, The hagfish pituitary gland and its putative adenohypophysial hormones. *Zool. Sci.* **25**, 1028–1036 (2008).
12. H. Kawauchi *et al.*, Identification of growth hormone in the sea lamprey, an extant representative of a group of the most ancient vertebrates. *Endocrinology* **143**, 4916–4921 (2002).
13. H. Kawauchi, S. A. Sower, The dawn and evolution of hormones in the adenohypophysis. *Gen. Comp. Endocrinol.* **148**, 3–14 (2006).
14. O. Simakov *et al.*, Deeply conserved synteny resolves early events in vertebrate evolution. *Nat. Ecol. Evol.* **4**, 820–830 (2020).
15. J. J. Smith, M. C. Keinath, The sea lamprey meiotic map improves resolution of ancient vertebrate genome duplications. *Genome Res.* **25**, 1081–1090 (2015).
16. Y. Nakatani *et al.*, Reconstruction of proto-vertebrate, proto-cyclostome and proto-gnathostome genomes provides new insights into early vertebrate evolution. *Nat. Commun.* **12**, 4489 (2021).
17. J. J. Smith *et al.*, The sea lamprey germline genome provides insights into programmed genome rearrangement and vertebrate evolution. *Nat. Genet.* **50**, 270–277 (2018).
18. T. K. Mehta *et al.*, Evidence for at least six Hox clusters in the Japanese lamprey (*Lethenteron japonicum*). *Proc. Natl. Acad. Sci. U.S.A.* **110**, 16044–16049 (2013).
19. T. Zhu *et al.*, Chromosome-level genome assembly of *Lethenteron reissneri* provides insights into lamprey evolution. *Mol. Ecol. Resour.* **21**, 448–463 (2021).
20. J. Pascual-Anaya *et al.*, Hagfish and lamprey Hox genes reveal conservation of temporal colinearity in vertebrates. *Nat. Ecol. Evol.* **2**, 859–866 (2018).
21. R. G. Manzon, J. H. Youson, J. A. Holmes, "Lamprey metamorphosis" in *Lampreys: Biology, Conservation and Control*, M. F. Docker, Ed. (Springer, 2015), pp. 139–195.
22. Y. Takei, S. D. McCormick, Hormonal control of fish euryhalinity. *Fish Physiol.* **32**, 69–123 (2012).
23. T. J. Marquis, M. Nozaki, W. Fagerberg, S. A. Sower, Comprehensive histological and immunological studies reveal a novel glycoprotein hormone and thyrostimulin expressing proto-glycotrope in the sea lamprey pituitary. *Cell Tissue Res.* **367**, 311–338 (2017).
24. M. Nozaki *et al.*, Identity and distribution of immunoreactive adenohypophysial cells in the pituitary during the life cycle of sea lampreys, *Petromyzon marinus*. *Gen. Comp. Endocrinol.* **155**, 403–412 (2008).
25. J. M. P. Joss, Pituitary control of metamorphosis in the southern hemisphere lamprey, Geotria australis. *Gen. Comp. Endocrinol.* **60**, 58–62 (1985).
26. N. Gong, D. Ferreira-Martins, S. D. McCormick, M. A. Sheridan, Divergent genes encoding the putative receptors for growth hormone and prolactin in sea lamprey display distinct patterns of expression. *Sci. Rep.* **10**, 1674 (2020).
27. Y. Shu *et al.*, The basal function of teleost prolactin as a key regulator on ion uptake identified with zebrafish knockout models. *Sci. Rep.* **6**, 18597 (2016).
28. R. Okada, M. Suzuki, N. Ito, S. Hyodo, S. Kikuyama, A novel type of prolactin expressed in the bullfrog pituitary specifically during the larval period. *Gen. Comp. Endocrinol.* **276**, 77–85 (2019).
29. H. Zhang *et al.*, Lampreys, the jawless vertebrates, contain only two ParaHox gene clusters. *Proc. Natl. Acad. Sci. U.S.A.* **114**, 9146–9151 (2017).
30. H. Qiu, F. Hildebrand, S. Kuraku, A. Meyer, Unresolved orthology and peculiar coding sequence properties of lamprey genes: The KCNA gene family as test case. *BMC Genomics* **12**, 325 (2011).
31. G. Hiyama *et al.*, Changes in post-translational modifications of prolactin during development and reproductive cycles in the chicken. *Gen. Comp. Endocrinol.* **161**, 238–245 (2009).
32. G. P. Baumann, Growth hormone isoforms. *Growth Horm. IGF Res.* **19**, 333–340 (2009).
33. A. L. Grigorian, J. J. Bustamante, P. Hernandez, A. O. Martinez, L. S. Haro, Extraordinarily stable disulfide-linked homodimer of human growth hormone. *Protein Sci.* **14**, 902–913 (2005).
34. A. L. M. Studzinski, D. V. Almeida, C. F. C. Lanes, Mde. A. Figueiredo, L. F. Marins, SOCS1 and SOCS3 are the main negative modulators of the somatotrophic axis in liver of homozygous GH-transgenic zebrafish (*Danio rerio*). *Gen. Comp. Endocrinol.* **161**, 67–72 (2009).
35. R. Laiz-Carrión, M. del Mar Segura-Noguera, M. del Pilar Martín del Río, J. M. Mancera, Ontogeny of adenohypophyseal cells in the pituitary of the American shad (*Alosa sapidissima*). *Gen. Comp. Endocrinol.* **132**, 454–464 (2003).
36. Y. Zhu *et al.*, Cloning of somatolactin alpha and beta cDNAs in zebrafish and phylogenetic analysis of two distinct somatolactin subtypes in fish. *J. Endocrinol.* **182**, 509–518 (2004).
37. X. Huang *et al.*, Discovery of a novel prolactin in non-mammalian vertebrates: Evolutionary perspectives and its involvement in teleost retina development. *PLoS One* **4**, e6163 (2009).
38. H. E. Bergan-Roller, M. A. Sheridan, The growth hormone signaling system: Insights into coordinating the anabolic and catabolic actions of growth hormone. *Gen. Comp. Endocrinol.* **258**, 119–133 (2018).
39. B. Th. Björnsson, I. E. Einarsdóttir, M. Johansson, N. Gong, The impact of initial energy reserves on growth hormone resistance and plasma growth hormone-binding protein levels in rainbow trout under feeding and fasting conditions. *Front. Endocrinol. (Lausanne)* **9**, 231 (2018).
40. N. Gong *et al.*, Roles of leptin in initiation of acquired growth hormone resistance and control of metabolism in rainbow trout. *Am. J. Physiol. Regul. Integr. Comp. Physiol.* **322**, R434–R444 (2022).
41. K. M. Reindl, J. D. Kittilson, H. E. Bergan, M. A. Sheridan, Growth hormone-stimulated insulin-like growth factor-1 expression in rainbow trout (*Oncorhynchus mykiss*) hepatocytes is mediated by ERK, PI3K-AKT, and JAK-STAT. *Am. J. Physiol. Regul. Integr. Comp. Physiol.* **301**, R236–R243 (2011).
42. T. Sakamoto, S. D. McCormick, Prolactin and growth hormone in fish osmoregulation. *Gen. Comp. Endocrinol.* **147**, 24–30 (2006).
43. D. Ferreira-Martins, J. M. Wilson, S. P. Kelly, D. Kolosov, S. D. McCormick, A review of osmoregulation in lamprey. *J. Great Lakes Res.* **47**, S59–S71 (2021).
44. C. A. Shaughnessy, S. D. McCormick, Functional characterization and osmoregulatory role of the Na^+-K^+-$2Cl^-$ cotransporter in the gill of sea lamprey (*Petromyzon marinus*), a basal vertebrate. *Am. J. Physiol. Regul. Integr. Comp. Physiol.* **318**, R17–R29 (2020).
45. D. Ferreira-Martins, J. Coimbra, C. Antunes, J. M. Wilson, Effects of salinity on upstream-migrating, spawning sea lamprey, *Petromyzon marinus*. *Conserv. Physiol.* **4**, cov064 (2016).
46. A. Barany *et al.*, Tissue and salinity specific Na^+/Cl^- cotransporter (NCC) orthologues involved in the adaptive osmoregulation of sea lamprey (*Petromyzon marinus*). *Sci. Rep.* **11**, 22698 (2021).
47. J. P. Breves, S. B. Serizier, V. Goffin, S. D. McCormick, R. O. Karlstrom, Prolactin regulates transcription of the ion uptake Na+/Cl- cotransporter (ncc) gene in zebrafish gill. *Mol. Cell. Endocrinol.* **369**, 98–106 (2013).
48. A. Larsson, AliView: A fast and lightweight alignment viewer and editor for large datasets. *Bioinformatics* **30**, 3276–3278 (2014).
49. M. Gouy, S. Guindon, O. Gascuel, SeaView version 4: A multiplatform graphical user interface for sequence alignment and phylogenetic tree building. *Mol. Biol. Evol.* **27**, 221–224 (2010).
50. D. Ocampo Daza, C. A. Bergqvist, D. Larhammar, The evolution of oxytocin and vasotocin receptor genes in jawed vertebrates: A clear case for gene duplications through ancestral whole-genome duplications. *Front. Endocrinol. (Lausanne)* **12**, 792644 (2022).
51. J. M. Mancera, S. D. McCormick, Evidence for growth hormone/insulin-like growth factor I axis regulation of seawater acclimation in the euryhaline teleost *Fundulus heteroclitus*. *Gen. Comp. Endocrinol.* **111**, 103–112 (1998).
52. S. D. McCormick, Effects of growth hormone and insulin-like growth factor I on salinity tolerance and gill Na+, K+-ATPase in Atlantic salmon (*Salmo salar*): Interaction with cortisol. *Gen. Comp. Endocrinol.* **101**, 3–11 (1996).
53. N. Gong, D. Ferreira-Martins, J. L. Norstog, S. D. McCormick, M. A. Sheridan, Data from "Discovery of prolactin-like in lamprey: Role in osmoregulation and new insight into the evolution of the growth hormone/prolactin family." Dryad. http://doi.org/10.5061/dryad.jdfn2z3dr. Deposited 29 August 2022.